AIAA 2013-5234

Nonlinear Adaptive Dynamic Inversion Applied to a Generic Hypersonic Vehicle

Elizabeth Rollins* and John Valasek†
Texas A&M University, College Station, TX 77843-3141
Jonathan A. Muse‡ and Michael A. Bolender§
U.S. Air Force Research Laboratory, Wright-Patterson Air Force Base, OH 45433

Flight control of hypersonic vehicles is challenging because of the wide range of operating conditions encountered and certain aspects unique to high speed flight. A particular safety concern in hypersonic flight is the risk of an inlet unstart, which not only produces a significant decrease in thrust but also results in a change to the aerodynamics and thus can lead to the loss of the vehicle. Previous work on control design for hypersonic vehicles often uses linearized or simplified nonlinear dynamical models of the vehicle, and very little work has been done on recovering from unstart events. Using a generic hypersonic vehicle as a control design and simulation model, this paper develops a nonlinear adaptive dynamic inversion control architecture with a control allocation scheme to track realistic flight path angle trajectories. A robustness analysis is performed on the initial control architecture design, which shows that the control architecture is able to handle time delays, perturbations in stability derivatives, and reduced control surface effectiveness. The control architecture then is evaluated for its ability to handle inlet unstart. Simulation results presented in the paper demonstrate that the approach achieves desired tracking performance while being robust to the particular uncertainties and inlet unstart conditions studied.

I. Introduction

The design of control architectures for hypersonic vehicles is a current area of research in the field of controls. One particular safety concern in hypersonic flight is the risk of an inlet unstart, which can lead to a decrease in thrust and the possible loss of the vehicle. There are three main reasons that cause a hypersonic airbreathing engine to unstart: (1) a flow to the inlet that is slower than the required Mach number for the engine to operate, (2) an altered flow that no longer passes through the throat of the engine because of reasons such as exceeding the limits on angle-of-attack (α) and sideslip angle (β), and (3) an increase in the back pressure in the engine that causes the shock wave to move ahead of the throat [1]. A control architecture for a hypersonic vehicle must be capable of maintaining the aircraft on a controlled trajectory in the event of an inlet unstart.

Many of the previous control designs for hypersonic vehicles have involved the use of linearized models of the aircraft instead of the full nonlinear equations of motion [2], [3], [4], [5]. Annaswamy, et.al. created adaptive controllers for hypersonic vehicles; however, the controllers are designed based on linearized models of the aircraft dynamics and require gain-scheduling for their implementation [2],[3]. Groves, et.al. implemented control designs based on linear models of a hypersonic vehicle for setpoint and regulator tracking [4]. Bolender, et.al. designed adaptive control laws for an experimental hypersonic vehicle based on a linearized model of the longitudinal dynamics of the vehicle [5].

In terms of work with nonlinear models for control design, Johnson, et.al. applied a neural network-based adaptive control architecture to a model of the X-33 vehicle for the generation of ascent and abort trajectories

*Graduate Student, Vehicle Systems & Controls Laboratory, AIAA Student Member, *erollins@tamu.edu.*
†Professor and Director, Vehicle Systems & Controls Laboratory, AIAA Associate Fellow, *valasek@tamu.edu, http://vscl.tamu.edu/valasek.*
‡Research Aerospace Engineer, AFRL/RQQA, and AIAA Member.
§Senior Research Engineer, AFRL/RQQA, and AIAA Associate Fellow.

as well as the control of the aircraft [6]. Fiorentini, et.al. [7] and Parker, et.al. [8] both used simplified nonlinear models of a hypersonic vehicle in their control design that exhibited good tracking performance but a slow response. While Parker, et.al. designed an approximate feedback linearization controller, the controller in that paper is not adaptive; however, a case study of their approximate feedback linearization controller showed that the controller was robust to mild plant parameter variations in the moment of inertia I_{yy}, the vehicle length, and the mass of the vehicle [9].

This paper presents a design of a nonlinear adaptive dynamic inversion controller for a Generic Hypersonic Vehicle (GHV). Because the dynamic equations for the GHV are inherently nonlinear and the aerodynamic and control derivatives for the aircraft have significant uncertainty associated with them, a nonlinear adaptive dynamic inversion control architecture was selected as the preferred control architecture. The design of the control architecture for the GHV involved the nonlinear equations of motion for the vehicle. When the reference trajectories were generated for the simulation, the adaptive dynamic inversion control architecture was altered to use altitude rate $\dot{h}$ instead of α, but the control architecture still used the nonlinear equation for $\dot{h}$ in its design.

The paper is organized as follows. Section II provides a brief overview of the GHV and the proposed control architecture. Section III contains the derivations of the general adaptive dynamic inversion equations that are used in the control architecture. Sections IV and V show how the nonlinear dynamic equations for the GHV are transformed into the form given in Section III for the control architecture. Representative simulation results and a robustness analysis of the nonlinear adaptive dynamic inversion control architecture are given in Section VI. Section VII describes the development of equations to allow realistic trajectories to be generated for the GHV simulation, and the simulation results for these realistic trajectories are shown in Section VIII. Finally, the conclusion and future extensions of this work are given in Section IX.

II. Control Structure for the GHV

The Generic Hypersonic Vehicle (GHV), as shown in Figure 1, is an academic hypersonic aircraft vehicle model created at the Air Force Research Laboratory as a platform for studying control laws. The GHV plant simulation is implemented using a Simulink model that contains the nonlinear, 6-DOF equations of motion for an inelastic hypersonic vehicle. The aerodynamic and thrust forces and moments acting on the vehicle are modeled using look-up tables; the tables for the aerodynamic forces and moments were generated based on computational fluid dynamics data using shock-expansion methods with a viscous correction.

Using two elevons and two ruddervators, it is desired to control angle-of-attack (α), sideslip angle (β), and aerodynamic bank angle (μ). It was decided to command the aerodynamic bank angle (μ) instead of the bank attitude angle (ϕ) in order to ensure that the dynamic inversion is singular only at $\beta = \pm 90$ deg. Figure 2 shows a diagram of the GHV system with the adaptive dynamic inversion controllers. To simplify the process of designing a nonlinear adaptive dynamic inversion control architecture, it is assumed that the aircraft states can be divided into two timescale categories, which are the fast states, which consist of the angular rates p, q, and r as noted in [10], and the slow states, which consist of the angles α, β, and μ. An adaptive dynamic inversion controller first must translate α, β, and μ commands into commands for the body axis rates p, q, and r, which then are passed into another adaptive dynamic inversion controller that determines the corresponding control surface deflections to achieve the desired p, q, and r commands.

The following three sections will describe the equations found in the inversion blocks in Figure 2. See Reference [11] for a description of the equations that are contained in the GHV simulation. For the equations derived in Sections IV and V, the flat, nonrotating earth assumption [12, p. 43] is made. It is acceptable to make this assumption in this case because while the vehicle is flying fast enough for the round rotating Earth effects to be significant, the time scale of the controlled dynamics are sufficiently fast to neglect them.

III. General Adaptive Dynamic Inversion Equations

This section contains the derivation of the control laws for two cases of the adaptive nonlinear dynamic inversion controller. The first case involves dynamic equations containing the same number of controls and controlled variables, and the second case deals with dynamic equations with a greater number of controls than controlled variables. It should be noted in both cases, the general nonlinear equation of the system is assumed to be affine in the control, which is reasonable for small deflection angles.

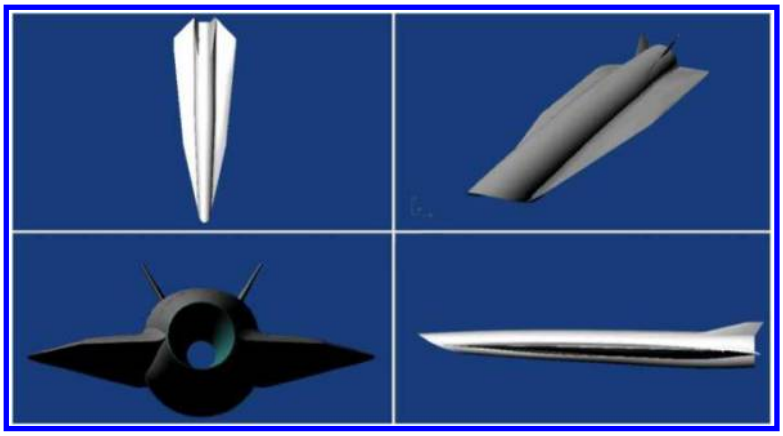

Figure 1. The Generic Hypersonic Vehicle (GHV).

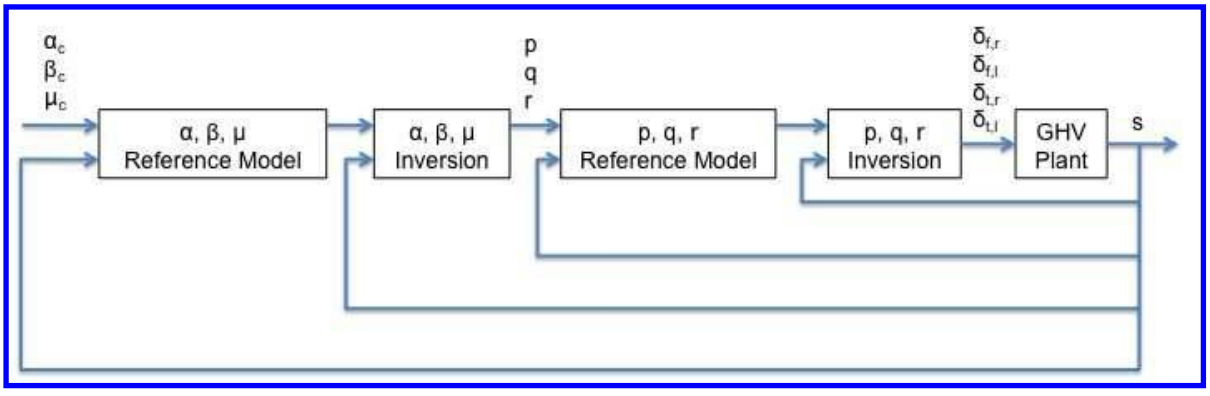

Figure 2. Diagram of the nonlinear adaptive dynamic inversion control architecture for the GHV.

A. Case with Equal Number of Controls and Controlled Variables

Consider a general nonlinear equation of a system in the form

$$\dot{x} = f(x) + g(x)u \tag{1}$$

where $x \in \mathbb{R}^n$ is the state, $u \in \mathbb{R}^n$ is the control, and $f(x) : \mathbb{R}^n \mapsto \mathbb{R}^n$ and $g(x) : \mathbb{R}^n \mapsto \mathbb{R}^n$ are locally Lipschitz continuous. It is assumed that $g(x)$ is nonsingular for all $x \in \mathbb{R}^n$. Suppose that the desired reference dynamics for the system are given by

$$\dot{x}_m = Ax_m + Br \tag{2}$$

where $x_m \in \mathbb{R}^n$ is the model state, $r \in \mathbb{R}^n$ is a bounded reference signal, $A \in \mathbb{R}^{n\times n}$ is Hurwitz, and $B \in \mathbb{R}^{n\times n}$. The equation for the error between the reference model and the actual system is

$$e = x_m - x. \tag{3}$$

Taking the time derivative of equation (3) results in

$$\dot{e} = \dot{x}_m - \dot{x} = \dot{x}_m - f(x) - g(x)u. \tag{4}$$

If the control u is chosen to be

$$u = [g(x)]^{-1}[\dot{x}_m - \hat{f}(x) + Ke - \nu] \tag{5}$$

where $\hat{f}(x) : \mathbb{R}^n \mapsto \mathbb{R}^n$ is a model of the plant dynamics, $K \in \mathbb{R}^{n\times n}$ such that $K = K^T > 0$ are the gains on the tracking errors, and $\nu \in \mathbb{R}^n$ is a pseudo-control signal, then substituting equation (5) into equation (4) produces the error dynamics

$$\dot{e} = -f(x) + \hat{f}(x) - Ke + \nu. \tag{6}$$

Defining the error between the model and the actual system as $\Delta = \hat{f}(x) - f(x)$, equation (6) becomes

$$\dot{e} = -Ke + \Delta + \nu. \tag{7}$$

In this paper, it is assumed that Δ can be represented in the form $\Delta = W^T\beta(x; d)$, where $W \in \mathbb{R}^{p\times n}$ is a set of unknown weights, and $\beta \in \mathbb{R}^{p\times 1}$ is a set of known basis functions composed of the states x and a vector d of bounded continuous exogenous inputs. Using this representation for Δ, ν is chosen to be $\nu = -\widehat{W}^T\beta(x; d)$, where $\widehat{W} \in \mathbb{R}^{p\times n}$ is an estimate of the weights. With these definitions, equation (7) can be written as

$$\dot{e} = -Ke - \widetilde{W}^T\beta(x; d) \tag{8}$$

where $\widetilde{W} = \widehat{W} - W$ is the weight estimation error.

The stability of the closed loop system under these assumptions can be established using a candidate Lyapunov function of the form

$$V = e^Te + tr(\widetilde{W}^T{\Gamma_W}^{-1}\widetilde{W}) \tag{9}$$

where $\Gamma_W \in \mathbb{R}^{p\times p}$ with $\Gamma_W = {\Gamma_W}^T > 0$. In order to determine the adaptation law for the parameters in W and to prove that the error between the states of the actual system and the reference model will converge, first, the derivative of equation (9) along the system trajectories is taken, which gives the result

$$\dot{V} = 2e^T\dot{e} + 2tr(\widetilde{W}^T{\Gamma_W}^{-1}\dot{\widehat{W}}^T). \tag{10}$$

Substituting equation (8) into equation (10) produces

$$\dot{V} = -2e^TKe - 2e^T\widetilde{W}^T\beta(x; d) + 2tr(\widetilde{W}^T{\Gamma_W}^{-1}\dot{\widehat{W}}^T). \tag{11}$$

Applying the trace identity that $a^Tb = tr(ba^T)$, equation (11) is determined to be

$$\dot{V} = -2e^TKe + 2tr(\widetilde{W}^T({\Gamma_W}^{-1}\dot{\widehat{W}}^T - \beta(x; d)e^T)). \tag{12}$$

Then, by choosing $\dot{\widehat{W}}$ as

$$\dot{\widehat{W}} = \Gamma_W Proj(\widehat{W}, \beta(x;d)e^T) \tag{13}$$

where Proj represents the projection operator, which is used to maintain specified bounds on the weights [13], $\dot{V}$ can be upper bounded as

$$\dot{V} \leq -2e^T Ke \leq 0 \tag{14}$$

which implies that e is bounded. Because r is bounded by definition above, x_m is bounded. Since e and x_m are bounded, x is bounded. Consequently, $\beta(x;d)$ is bounded as well. In order to use Barbalat's lemma [14] to complete the proof, the second derivative of equation (9) along the system trajectories is taken, which gives the result

$$\ddot{V} = -4e^T K\dot{e}. \tag{15}$$

Substituting equation (8) into equation (15) produces

$$\ddot{V} = -4e^T K(-Ke - \widetilde{W}^T\beta(x;d)). \tag{16}$$

Because e, $\widetilde{W}$, and $\beta(x;d)$ are bounded as proved above, $\ddot{V}$ is bounded, and therefore $\dot{V}$ is uniformly continuous.

Because V is lower bounded, $\dot{V}$ is negative semi-definite, and $\dot{V}$ is uniformly continuous, by Barbalat's lemma $\dot{V} \to 0$ as $t \to \infty$, and thus $e \to 0$ as $t \to \infty$ as desired.

B. Case with a Greater Number of Controls Than Controlled Variables

Specifically for the GHV, the form of the general adaptive dynamic inversion controller in the previous subsection applies to the α, β, and μ inversion component, in which the number of inputs to the system (α, β, μ) is equal to the number of outputs (p, q, r). However, in the p, q, r inversion component, the number of inputs to the system (p, q, r) is not the same as the number of outputs ($\delta_{f,r}$, $\delta_{f,l}$, $\delta_{t,r}$, $\delta_{t,l}$). The fact that the number of outputs is greater than the number of inputs requires a control allocation scheme to be integrated into the inversion control law. To frame the problem in general terms, consider the given nonlinear equation of a system in the form

$$\dot{x} = f(x) + g(x)\Lambda u \tag{17}$$

where $x \in \mathbb{R}^n$ is the state, $u \in \mathbb{R}^m$ is the control, $f(x) : \mathbb{R}^n \mapsto \mathbb{R}^n$ and $g(x) : \mathbb{R}^n \mapsto \mathbb{R}^{n\times m}$ are locally Lipschitz continuous, and $\Lambda \in \mathbb{R}^{m\times m}$ is a constant unknown positive definite matrix. It is assumed that $g(x)$ is full rank for all $x \in \mathbb{R}^n$. Suppose that the desired dynamics of the closed loop system are given by

$$\dot{x}_m = Ax_m + Br \tag{18}$$

where $x_m \in \mathbb{R}^n$ is the model state, $r \in \mathbb{R}^m$ is the bounded reference signal, $A \in \mathbb{R}^{n\times n}$ is Hurwitz, and $B \in \mathbb{R}^{n\times m}$.

The derivation of the control law and the adaptive laws, including one for the unknown control effectiveness matrix Λ, proceeds similarly to the derivation in Subsection A. The equation for the error between the reference model and the actual system is

$$e = x_m - x. \tag{19}$$

Taking the time derivative of equation (19) results in

$$\dot{e} = \dot{x}_m - \dot{x} = \dot{x}_m - f(x) - g(x)\Lambda u. \tag{20}$$

The desired final form for $\dot{e}$ is

$$\dot{e} = -Ke - \widetilde{W}^T\beta(x;d) + g(x)\widetilde{\Lambda}u \tag{21}$$

which is the same as the final form for $\dot{e}$ in Subsection A, except for the final term $g(x)\widetilde{\Lambda}u$. With the appropriate choice of adaptive law for $\widehat{\Lambda}$, the choice of the above final form for $\dot{e}$ will allow the stability of the system to be proven. In order to derive this desired form of $\dot{e}$, first the term $g(x)\widehat{\Lambda}u$ is added and subtracted from equation (20), where $\widehat{\Lambda} \in \mathbb{R}^{m\times m}$ is an estimate of the control effectiveness matrix, and the error equation becomes

$$\dot{e} = \dot{x}_m - f(x) - g(x)\Lambda u + g(x)\widehat{\Lambda}u - g(x)\widehat{\Lambda}u. \tag{22}$$

Let $\widetilde{\Lambda} = \widehat{\Lambda} - \Lambda$, which is the estimation error of the control effectiveness matrix. Then, equation (22) simplifies to

$$\dot{e} = \dot{x}_m - f(x) - g(x)\widehat{\Lambda}u + g(x)\widetilde{\Lambda}u. \tag{23}$$

Because of the fact that the number of controls is greater than the number of controlled variables in this case, there sometimes are infinite choices for u at any instant in time. In order to determine a specific control law for the system, a constrained optimization problem is solved in which the cost function $J = u^T Q u$, where $Q \in \mathbb{R}^{m\times m}$ with $Q = Q^T > 0$, will be minimized, subject to the constraint $g(x)\widehat{\Lambda}u = \ell$, which must be satisfied at all times. The cost function is chosen to be $J = u^T Q u$ so that the control effort will be minimized, which consequently can be used to reduce the amount of trim drag during flight. it is assumed by this formulation of the problem that the control surfaces do not have position limits, and as a result, sufficient control power will always exist. By choosing the term ℓ in the constraint equation to be

$$\ell = \dot{x}_m - \hat{f}(x) + Ke - \nu \tag{24}$$

where $\hat{f}(x) : \mathbb{R}^n \mapsto \mathbb{R}^n$ is an estimate of the plant dynamics, $K \in \mathbb{R}^{n\times n}$ with $K = K^T > 0$ contains the gains on the errors, and $\nu \in \mathbb{R}^n$ is a pseudo-control signal, the constraint $g(x)\widehat{\Lambda}u = \ell$ will ensure that when the derived control law for this second case is substituted into the equation for $\dot{e}$, and the equation for the error dynamics is simplified, the first two terms of equation (21) will appear in the resulting equation for $\dot{e}$ as desired. For simplicity in the control law derivation, equation (24) will not be substituted into the constraint equation at the present time.

To derive the control law, first the constraint must be included in the cost function to form the augmented cost function

$$\bar{J} = u^T Q u + \lambda^T (g(x)\widehat{\Lambda}u - \ell) \tag{25}$$

where $\lambda \in \mathbb{R}^n$ is a Lagrange multiplier. The necessary conditions for minimizing $\bar{J}$ are given by

$$\frac{\partial \bar{J}}{\partial \lambda} = g(x)\widehat{\Lambda}u - \ell = 0 \tag{26}$$

$$\frac{\partial \bar{J}}{\partial u} = 2Qu + \widehat{\Lambda}^T g^T(x)\lambda = 0. \tag{27}$$

Rearranging terms in equation (27) results in

$$u = -\frac{1}{2}Q^{-1}\widehat{\Lambda}^T g^T(x)\lambda. \tag{28}$$

Substituting equation (28) into equation (26) and solving for λ produces the equation

$$\lambda = -2(g(x)\widehat{\Lambda}Q^{-1}\widehat{\Lambda}^T g^T(x))^{-1}\ell. \tag{29}$$

Finally, substituting equation (29) back into equation (28) results in the control law

$$u = Q^{-1}\widehat{\Lambda}^T g^T(x)(g(x)\widehat{\Lambda}Q^{-1}\widehat{\Lambda}^T g^T(x))^{-1}\ell. \tag{30}$$

In order for the control law given in equation (30) to be continuous, Q and $g(x)\widehat{\Lambda}Q^{-1}\widehat{\Lambda}^T g^T(x)$ must be invertible. The projection bounds that will be applied in the adaptive law for Λ must ensure that $\widehat{\Lambda}$ remains invertible. It should be noted that for the case where the number of controls equals the number of controlled variables, the control solution is unique, and the control law in equation (30) simplifies to

$$u = [g(x)]^{-1}[\dot{x}_m - \hat{f}(x) + Ke - \nu] \tag{31}$$

which is the control law that was chosen in Subsection A.

Continuing with the derivation of $\dot{e}$, let $\Delta = \hat{f}(x) - f(x)$. Substituting equation (30), equation (24), and into equation (23) produces the equation

$$\dot{e} = -Ke + \Delta + \nu + g(x)\widetilde{\Lambda}u. \tag{32}$$

Again, assume that Δ can be represented in the form $\Delta = W^T\beta(x;d)$, where $W \in \mathbb{R}^{p\times n}$ is a set of unknown weights, and $\beta \in \mathbb{R}^{p\times 1}$ is a set of known basis functions composed of the states x and a vector d

of bounded continuous exogenous inputs. Also, the representation for ν is chosen to be $\nu = -\widehat{W}^T\beta(x;d)$, where $\widehat{W} \in \mathbb{R}^{p\times n}$. Then, equation (32) can be written as

$$\dot{e} = -Ke - \widetilde{W}^T\beta(x;d) + g(x)\widetilde{\Lambda}u \tag{33}$$

where $\widetilde{W} = \widehat{W} - W$, which is the weight estimation error.

As in Subsection A, a Lyapunov analysis needs to be performed in order to determine the adaptive laws for $\widehat{\Lambda}$ and $\widehat{W}$ and to prove that the error between the states of the actual system and the reference model will converge. Given the candidate Lyapunov function

$$V = e^Te + tr(\widetilde{W}^T{\Gamma_W}^{-1}\widetilde{W}) + tr(\widetilde{\Lambda}{\Gamma_\Lambda}^{-1}\widetilde{\Lambda}) \tag{34}$$

where $\Gamma_W \in \mathbb{R}^{p\times p}$ with $\Gamma_W = {\Gamma_W}^T > 0$, and $\Gamma_\Lambda \in \mathbb{R}^{m\times m}$ with $\Gamma_\Lambda = {\Gamma_\Lambda}^T > 0$, the derivative of equation (34) along the system trajectories is taken, which results in the equation

$$\dot{V} = 2e^T\dot{e} + 2tr(\widetilde{W}^T{\Gamma_W}^{-1}\dot{\widehat{W}}^T) + 2tr(\widetilde{\Lambda}{\Gamma_\Lambda}^{-1}\dot{\widehat{\Lambda}}^T). \tag{35}$$

Substituting equation (33) into equation (35) produces

$$\dot{V} = -2e^TKe - 2e^T\widetilde{W}^T\beta(x;d) + 2e^Tg(x)\widetilde{\Lambda} + 2tr(\widetilde{W}^T{\Gamma_W}^{-1}\dot{\widehat{W}}^T) + 2tr(\widetilde{\Lambda}{\Gamma_\Lambda}^{-1}\dot{\widehat{\Lambda}}^T) \tag{36}$$

and by applying the trace identity that $a^Tb = tr(ba^T)$ to equation (36), the equation for $\dot{V}$ becomes

$$\dot{V} = -2e^TKe + 2tr(\widetilde{W}^T({\Gamma_W}^{-1}\dot{\widehat{W}}^T - \beta(x;d)e^T)) + 2tr(\widetilde{\Lambda}({\Gamma_\Lambda}^{-1}\dot{\widehat{\Lambda}}^T + ue^Tg(x))). \tag{37}$$

Let the equation for $\dot{\widehat{W}}$ in this case be the same as equation (13), and let $\dot{\widehat{\Lambda}}$ be

$$\dot{\widehat{\Lambda}} = \Gamma_\Lambda Proj(\widehat{\Lambda}, -ue^Tg(x)). \tag{38}$$

In this case, the final equation for $\dot{V}$ is is upper bounded by

$$\dot{V} \leq -2e^TKe \leq 0 \tag{39}$$

which implies that e is bounded. Since r is bounded by definition above and e is bounded, x_m is bounded, and thus x is bounded. Consequently, $g(x)$ and $\beta(x;d)$ are bounded as well. In order to use Barbalat's lemma to complete the proof, the second derivative of equation (34) along the system trajectories is taken, which gives the result

$$\ddot{V} = -4e^TK\dot{e}. \tag{40}$$

Substituting equation (33) into equation (40) produces

$$\ddot{V} = -4e^TK(-Ke - \widetilde{W}^T\beta(x;d) + g(x)\widetilde{\Lambda}u). \tag{41}$$

It should be noted that u is bounded because all of the the signals found in u, which is given by equations (30) and (24) are bounded. Thus, because e, $\widetilde{W}$, $\beta(x;d)$, $g(x)$, $\widetilde{\Lambda}$, and u are bounded as proved above, $\ddot{V}$ is bounded, and therefore $\dot{V}$ is uniformly continuous.

Finally, Barbalat's lemma can be applied. Because V is lower bounded, $\dot{V}$ is negative semi-definite, and $\dot{V}$ is uniformly continuous, by Barbalat's lemma $\dot{V} \to 0$ as $t \to \infty$, and thus $e \to 0$ as $t \to \infty$ as desired.

IV. P, Q, R Inversion Controller

The first designed controller was the inversion controller for the angular body rates of the GHV since these variables are linked directly to the control surface deflections, which control the vehicle. The reference inputs to the controller are the commanded angular body rates p_c, q_c and r_c, and the output states of the controller are the control surface deflections $\delta_{f,r}$, $\delta_{f,l}$, $\delta_{t,r}$, and $\delta_{t,l}$. Therefore, in this case, equation (17) represents the current system. In order for the adaptive dynamic inversion controller to be designed for the

angular body rates, $f(x)$ and $g(x)$ must be determined from the general nonlinear equations for $\dot{p}$, $\dot{q}$, and $\dot{r}$, which in vector-matrix form, are

$$[J]\frac{d\omega_{B,I}}{dt}\bigg|_B + \omega_{B,I} \times J\omega_{B,I} = M_{aero} + M_T \tag{42}$$

where

$$[J] = \begin{bmatrix} J_x & 0 & -J_{xz} \\ 0 & J_y & 0 \\ -J_{xz} & 0 & J_z \end{bmatrix} \tag{43}$$

and

$$\omega_{B,I} = \begin{bmatrix} p \\ q \\ r \end{bmatrix}. \tag{44}$$

Substituting these equations into equation (42) and simplifying produces the result

$$\begin{bmatrix} J_x & 0 & -J_{xz} \\ 0 & J_y & 0 \\ -J_{xz} & 0 & J_z \end{bmatrix} \begin{bmatrix} \dot{p} \\ \dot{q} \\ \dot{r} \end{bmatrix} + \begin{bmatrix} -J_{xz}pq + (J_z - J_y)qr \\ (J_x - J_z)pr + J_{xz}(p^2 - r^2) \\ J_{xz}qr + (J_y - J_x)pq \end{bmatrix} = M_{aero} + M_T. \tag{45}$$

Therefore, the nonlinear equations for the angular body accelerations can be written as

$$\begin{bmatrix} \dot{p} \\ \dot{q} \\ \dot{r} \end{bmatrix} = \begin{bmatrix} J_x & 0 & -J_{xz} \\ 0 & J_y & 0 \\ -J_{xz} & 0 & J_z \end{bmatrix}^{-1} \left(- \begin{bmatrix} -J_{xz}pq + (J_z - J_y)qr \\ (J_x - J_z)pr + J_{xz}(p^2 - r^2) \\ J_{xz}qr + (J_y - J_x)pq \end{bmatrix} + M_{aero} + M_T \right). \tag{46}$$

After having determined the nonlinear equations for the angular body accelerations, the next step is to write those equations in the form of equation (17). In order to accomplish this task, the terms related to the control surfaces, which will form $g(x)$, must be extracted from equation (46). The control surfaces terms are included in the aerodynamic moment terms M_A, which are modeled as

$$M_{aero} = \begin{bmatrix} L_A \\ M_A \\ N_A \end{bmatrix} = \begin{bmatrix} \bar{q}SbC_\ell \\ \bar{q}S\bar{c}C_m \\ \bar{q}SbC_n \end{bmatrix} \tag{47}$$

where

$$\begin{aligned} C_\ell &= C_{\ell,baseline} + \Delta C_{\ell,surfaces} + \frac{b}{2V_T}\left(C_{\ell_p}p\right) \\ C_m &= C_{m,baseline} + \Delta C_{m,surfaces} + \frac{\bar{c}}{2V_T}\left(C_{m_q}q + C_{m_{\dot{\alpha}}}\dot{\alpha}\right) \\ C_n &= C_{n,baseline} + \Delta C_{n,surfaces} + \frac{b}{2V_T}\left(C_{n_r}r\right) \end{aligned} \tag{48}$$

and

$$\begin{aligned} \Delta C_{i,surfaces} = {} & \Delta C_{i,\delta_{f,r}}(M,\alpha,\beta,\delta_{f,r}) + \Delta C_{i,\delta_{f,l}}(M,\alpha,\beta,\delta_{f,l}) \\ & + \Delta C_{i,\delta_{t,r}}(M,\alpha,\beta,\delta_{t,r}) + \Delta C_{i,\delta_{t,l}}(M,\alpha,\beta,\delta_{t,l}) \end{aligned} \tag{49}$$

for $i = \ell$, m, n.

As seen in equation (48), the moment coefficients are comprised of three parts. The baseline term is the moment coefficient for the base airframe, while the second and third terms adjust for the effects on the moment coefficients due to the control surfaces and damping, respectively. In equation (48), the first and third terms do not depend on the control surfaces; therefore, those two terms belong to the $f(x)$ term in equation (17). In order to determine $g(x)$, the second term in each equation in equation (48) must be examined to determine what portion of the term is control-dependent and thus belongs in $g(x)$. For this particular control design for the GHV, it is assumed that a linear approximation with respect to the control

surface deflection δ can be made for each of the terms in equation (49). The linear approximation can be expressed as

$$\begin{aligned}\Delta C_{i,\delta_s}(M,\alpha,\beta,\delta_s) &= C_{i,\delta_s}(M,\alpha,\beta,[\delta_s=0]) + \left.\frac{\partial C_{i,\delta_s}}{\partial \delta_s}\right|_{M,\alpha,\beta \text{ constant}} \Delta\delta_s \\ &\text{for } i = N, Y, A, \ell, m, n \\ &\text{and } \delta_s = \delta_{f,r}, \delta_{f,l}, \delta_{t,r}, \delta_{t,l}.\end{aligned} \tag{50}$$

In this paper, it is assumed that all interactions between each control surface are negligible, which at high Mach numbers is approximately true. Deflections of the right and left control surfaces will generate summative forces and moments in the XZ-plane of symmetry of the aircraft, whereas in the other planes, the deflections will generate canceling forces and moments. In equation form, for both the flaps and the tail control surfaces, the relationships between right and left elevon deflections are expressed as

$$\begin{aligned} C_{N,\delta_{f,r}} &= C_{N,\delta_{f,l}} & -C_{Y,\delta_{f,r}} &= C_{Y,\delta_{f,l}} \\ C_{A,\delta_{f,r}} &= C_{A,\delta_{f,l}} & -C_{\ell,\delta_{f,r}} &= C_{\ell,\delta_{f,l}} \\ C_{m,\delta_{f,r}} &= C_{m,\delta_{f,l}} & -C_{n,\delta_{f,r}} &= C_{n,\delta_{f,l}} \end{aligned} \tag{51}$$

and the relationships between right and left rudder deflections are expressed similarly as

$$\begin{aligned} C_{N,\delta_{t,r}} &= C_{N,\delta_{t,l}} & -C_{Y,\delta_{t,r}} &= C_{Y,\delta_{t,l}} \\ C_{A,\delta_{t,r}} &= C_{A,\delta_{t,l}} & -C_{\ell,\delta_{t,r}} &= C_{\ell,\delta_{t,l}} \\ C_{m,\delta_{t,r}} &= C_{m,\delta_{t,l}} & -C_{n,\delta_{t,r}} &= C_{n,\delta_{t,l}}. \end{aligned} \tag{52}$$

Consequently, in equation (50), the term where $\delta_s = 0$ can be written for the combined effect of both the right and left control surfaces collectively as

$$C_{i,\delta_f}(M,\alpha,\beta,[\delta_{f,r}=0,\delta_{f,l}=0]) = \begin{cases} 2C_{i,\delta_{f,r}}(M,\alpha,\beta,[\delta_{f,r}=0]) & \text{for } i = N, A, m \\ 0 & \text{for } i = Y, \ell, n \end{cases} \tag{53}$$

$$C_{i,\delta_t}(M,\alpha,\beta,[\delta_{t,r}=0,\delta_{t,l}=0]) = \begin{cases} 2C_{i,\delta_{t,r}}(M,\alpha,\beta,[\delta_{t,r}=0]) & \text{for } i = N, A, m \\ 0 & \text{for } i = Y, \ell, n. \end{cases} \tag{54}$$

Given equations (50), (53), and (54), equation (49) can be rewritten for $i = \ell, m, n$ as

$$\begin{aligned}\Delta C_\ell = &\left.\frac{\partial C_{\ell,\delta_{f,r}}}{\partial \delta_{f,r}}\right|_{M,\alpha,\beta \text{ constant}} \Delta\delta_{f,r} + \left.\frac{\partial C_{\ell,\delta_{f,l}}}{\partial \delta_{f,l}}\right|_{M,\alpha,\beta \text{ constant}} \Delta\delta_{f,l} \\ &+ \left.\frac{\partial C_{\ell,\delta_{t,r}}}{\partial \delta_{t,r}}\right|_{M,\alpha,\beta \text{ constant}} \Delta\delta_{t,r} + \left.\frac{\partial C_{\ell,\delta_{t,l}}}{\partial \delta_{t,l}}\right|_{M,\alpha,\beta \text{ constant}} \Delta\delta_{t,l}\end{aligned} \tag{55}$$

$$\begin{aligned}\Delta C_m = &\, 2C_{m,\delta_{f,r}}(M,\alpha,\beta,[\delta_{f,r}=0]) + 2C_{m,\delta_{t,r}}(M,\alpha,\beta,[\delta_{t,r}=0]) \\ &+ \left.\frac{\partial C_{m,\delta_{f,r}}}{\partial \delta_{f,r}}\right|_{M,\alpha,\beta \text{ constant}} \Delta\delta_{f,r} + \left.\frac{\partial C_{m,\delta_{f,l}}}{\partial \delta_{f,l}}\right|_{M,\alpha,\beta \text{ constant}} \Delta\delta_{f,l} \\ &+ \left.\frac{\partial C_{m,\delta_{t,r}}}{\partial \delta_{t,r}}\right|_{M,\alpha,\beta \text{ constant}} \Delta\delta_{t,r} + \left.\frac{\partial C_{m,\delta_{t,l}}}{\partial \delta_{t,l}}\right|_{M,\alpha,\beta \text{ constant}} \Delta\delta_{t,l}\end{aligned} \tag{56}$$

$$\begin{aligned}\Delta C_n = &\left.\frac{\partial C_{n,\delta_{f,r}}}{\partial \delta_{f,r}}\right|_{M,\alpha,\beta \text{ constant}} \Delta\delta_{f,r} + \left.\frac{\partial C_{n,\delta_{f,l}}}{\partial \delta_{f,l}}\right|_{M,\alpha,\beta \text{ constant}} \Delta\delta_{f,l} \\ &+ \left.\frac{\partial C_{n,\delta_{t,r}}}{\partial \delta_{t,r}}\right|_{M,\alpha,\beta \text{ constant}} \Delta\delta_{t,r} + \left.\frac{\partial C_{n,\delta_{t,l}}}{\partial \delta_{t,l}}\right|_{M,\alpha,\beta \text{ constant}} \Delta\delta_{t,l}.\end{aligned} \tag{57}$$

Since the first two terms of equation (56) are for fixed values of δ_s, they constitute bias terms and therefore belong in the $f(x)$ portion of equation (17). As a result, only the terms represented by $\left.\frac{\partial C_{i,\delta_s}}{\partial \delta_s}\right|_{M,\alpha,\beta \text{ constant}}$ in equations (55), (56), and (57) belong in the $g(x)$ term in equation (17).

To complete the analysis of the terms in equation (46), the effect of the center of gravity shift must be accounted for in the nonlinear equations for the angular body accelerations. The shift of a set of moments from a given reference point to the center of gravity is given by the equation

$$M_{cg} = M_{aero} - r_{cg/aero} \times F_{aero} \tag{58}$$

and in this particular simulation, $r_{cg/aero}$ is defined to be $\begin{bmatrix} x_{cg} & 0 & 0 \end{bmatrix}^T$. In the simulation, F_{aero} is calculated similarly to M_{aero} in equation (47) above, which means that F_{aero} has the form

$$F_{aero} = \begin{bmatrix} X_A \\ Y_A \\ Z_A \end{bmatrix} = \begin{bmatrix} -\bar{q}SC_A \\ \bar{q}SC_Y \\ -\bar{q}SC_N \end{bmatrix}. \tag{59}$$

Therefore, given equation (59) and the definition of $r_{cg/aero}$, equation (58) can be written as

$$M_{cg} = M_{aero} - \begin{bmatrix} x_{cg} \\ 0 \\ 0 \end{bmatrix} \times \begin{bmatrix} -\bar{q}SC_A \\ \bar{q}SC_Y \\ -\bar{q}SC_N \end{bmatrix} \tag{60}$$

$$M_{cg} = M_{aero} - \begin{bmatrix} 0 \\ -\bar{q}SC_N x_{cg} \\ -\bar{q}SC_Y x_{cg} \end{bmatrix} \tag{61}$$

where M_{aero} is defined in equation (47). It should be noted that the terms C_N and C_Y in equation (61) can be written like the moment coefficients in equations (55), (56), and (57) as

$$\begin{aligned} \Delta C_N = {} & 2C_{N,\delta_{f,r}}(M,\alpha,\beta,[\delta_{f,r}=0]) + 2C_{N,\delta_{t,r}}(M,\alpha,\beta,[\delta_{t,r}=0]) \\ & + \left.\frac{\partial C_{N,\delta_{f,r}}}{\partial \delta_{f,r}}\right|_{M,\alpha,\beta \text{ constant}} \Delta\delta_{f,r} + \left.\frac{\partial C_{N,\delta_{f,l}}}{\partial \delta_{f,l}}\right|_{M,\alpha,\beta \text{ constant}} \Delta\delta_{f,l} \\ & + \left.\frac{\partial C_{N,\delta_{t,r}}}{\partial \delta_{t,r}}\right|_{M,\alpha,\beta \text{ constant}} \Delta\delta_{t,r} + \left.\frac{\partial C_{N,\delta_{t,l}}}{\partial \delta_{t,l}}\right|_{M,\alpha,\beta \text{ constant}} \Delta\delta_{t,l} \end{aligned} \tag{62}$$

$$\begin{aligned} \Delta C_Y = {} & \left.\frac{\partial C_{Y,\delta_{f,r}}}{\partial \delta_{f,r}}\right|_{M,\alpha,\beta \text{ constant}} \Delta\delta_{f,r} + \left.\frac{\partial C_{Y,\delta_{f,l}}}{\partial \delta_{f,l}}\right|_{M,\alpha,\beta \text{ constant}} \Delta\delta_{f,l} \\ & + \left.\frac{\partial C_{Y,\delta_{t,r}}}{\partial \delta_{t,r}}\right|_{M,\alpha,\beta \text{ constant}} \Delta\delta_{t,r} + \left.\frac{\partial C_{Y,\delta_{t,l}}}{\partial \delta_{t,l}}\right|_{M,\alpha,\beta \text{ constant}} \Delta\delta_{t,l} \end{aligned} \tag{63}$$

Similarly to the moment coefficients as shown above, since the first two terms of equation (62) are for fixed values of δ_s, they constitute bias terms and therefore belong in the $f(x)$ portion of equation (17). As a result, only the terms represented by $\left.\frac{\partial C_{i,\delta_s}}{\partial \delta_s}\right|_{M,\alpha,\beta \text{ constant}}$ in equations (62) and (63) belong in the $g(x)$ term in equation (17).

Having examined all of the terms in the nonlinear equations for the angular body accelerations, equation (46) can be written in the final form of equation (17) as

$$\begin{bmatrix} \dot{p} \\ \dot{q} \\ \dot{r} \end{bmatrix} = \begin{bmatrix} J_x & 0 & -J_{xz} \\ 0 & J_y & 0 \\ -J_{xz} & 0 & J_z \end{bmatrix}^{-1} \left(- \begin{bmatrix} -J_{xz}pq + (J_z - J_y)qr \\ (J_x - J_z)pr + J_{xz}(p^2 - r^2) \\ J_{xz}qr + (J_y - J_x)pq \end{bmatrix} + M_T + \bar{q}SG + \bar{q}SH \begin{bmatrix} \delta_{f,r} \\ \delta_{f,l} \\ \delta_{t,r} \\ \delta_{t,l} \end{bmatrix} \right) \tag{64}$$

where

$$G = \begin{bmatrix} b\left(C_{\ell,baseline} + \frac{b}{2V_T}(C_{\ell_p}p)\right) \\ \bar{c}\left(C_{m,baseline} + \frac{\bar{c}}{2V_T}(C_{m_q}q + C_{m_{\dot{\alpha}}}\dot{\alpha}) + 2C_{m,\delta_{f,r}}(\delta_{f,r}=0) + 2C_{m,\delta_{t,r}}(\delta_{t,r}=0)\right) \\ -2C_{N,\delta_{f,r}}(\delta_{f,r}=0)x_{cg} - 2C_{N,\delta_{t,r}}(\delta_{t,r}=0)x_{cg} \\ b\left(C_{r,baseline} + \frac{b}{2V_T}(C_{n_r}r)\right) \end{bmatrix} \tag{65}$$

and

$$H = \begin{bmatrix} b\frac{\partial C_\ell}{\partial \delta_{f,r}} & b\frac{\partial C_\ell}{\partial \delta_{f,l}} & b\frac{\partial C_\ell}{\partial \delta_{t,r}} & b\frac{\partial C_\ell}{\partial \delta_{t,l}} \\ \left(\bar{c}\frac{\partial C_m}{\partial \delta_{f,r}} - x_{cg}\frac{\partial C_N}{\partial \delta_{f,r}}\right) & \left(\bar{c}\frac{\partial C_m}{\partial \delta_{f,l}} - x_{cg}\frac{\partial C_N}{\partial \delta_{f,l}}\right) & \left(\bar{c}\frac{\partial C_m}{\partial \delta_{t,r}} - x_{cg}\frac{\partial C_N}{\partial \delta_{t,r}}\right) & \left(\bar{c}\frac{\partial C_m}{\partial \delta_{t,l}} - x_{cg}\frac{\partial C_N}{\partial \delta_{t,l}}\right) \\ \left(b\frac{\partial C_n}{\partial \delta_{f,r}} - x_{cg}\frac{\partial C_Y}{\partial \delta_{f,r}}\right) & \left(b\frac{\partial C_n}{\partial \delta_{f,l}} - x_{cg}\frac{\partial C_Y}{\partial \delta_{f,l}}\right) & \left(b\frac{\partial C_n}{\partial \delta_{t,r}} - x_{cg}\frac{\partial C_Y}{\partial \delta_{t,r}}\right) & \left(b\frac{\partial C_n}{\partial \delta_{t,l}} - x_{cg}\frac{\partial C_Y}{\partial \delta_{t,l}}\right) \end{bmatrix}. \tag{66}$$

It should be noted that the partial derivatives in equation (64) are taken with respect to a constant value of M, α, and β from the current flight condition and that the control surface bias terms, where $\delta_s = 0$, are evaluated at a constant value of M, α and β from the current flight condition as well.

Given equation (64), which is now in the form of equation (17), the adaptive dynamic inversion controller can be constructed using equations (13), (24), (30), and (38).

V. α, β, μ Inversion Controller

As with the p, q, r inversion controller, equations for $\dot{\alpha}$, $\dot{\beta}$, and $\dot{\mu}$ must be determined in order for the adaptive dynamic inversion controller to be constructed. It should be noted that for this section, S_x will represent $\sin(x)$, C_x will represent $\cos(x)$, and T_x will represent $\tan(x)$, where x is an angle. The derivations for $\dot{\alpha}$ and $\dot{\beta}$ are based on the derivations for those terms on pages 110-112 in Reference [15]. The starting point of the derivations is the basic force equations in the stability axes under the flat Earth assumption, which are

$${}^b\dot{v}_{rel} = (1/m)F_{A,T} + g - \omega_{b/e} \times v_{rel}. \tag{67}$$

Taking the time derivative of the relative velocity in the wind axes instead of in the body axes and converting the right hand side of equation (67) to the wind axes produces the result

$$m\dot{V}_T = F_T C_{\alpha+\alpha_T} C_\beta - D - mgS_\gamma \tag{68}$$

$$m\dot{\beta}V_T = -F_T C_{\alpha+\alpha_T} S_\beta - C + mg(C_\alpha S_\beta S_\theta + C_\beta S_\phi C_\theta - S_\alpha S_\beta C_\phi C_\theta) - mV_T(pS_\alpha - rC_\alpha) \tag{69}$$

$$m\dot{\alpha}V_T C_\beta = -F_T S_{\alpha+\alpha_T} - L + mg(S_\alpha S_\theta + C_\alpha C_\phi C_\theta) + mV_T(-pS_\beta C_\alpha + qC_\beta - rS_\beta S_\alpha) \tag{70}$$

where D, L, and C represent drag, lift, and cross-wind force, respectively, in the wind axes.

In order to simplify equations (69) and (70) and to express them in terms of μ, which is one of the commanded states, the gravity terms in those equations are transformed using relationships given by the following direction cosine matrices from Chapter 4 of Reference [12] as

$$T_{W,H}(\mu,\gamma,\chi) = T^T_{B,W}(0,-\alpha,\beta)T_{B,H}(\phi,\theta,\psi) \tag{71}$$

where W represents the wind axes, B represents the body axes, and H represents the local horizon axes. Each direction cosine matrix has the general form

$$T_{2,1}(\theta_x,\theta_y,\theta_z) = \begin{bmatrix} C_{\theta_y}C_{\theta_z} & C_{\theta_y}S_{\theta_z} & -S_{\theta_y} \\ S_{\theta_x}S_{\theta_y}C_{\theta_z} - C_{\theta_x}S_{\theta_z} & S_{\theta_x}S_{\theta_y}S_{\theta_z} + C_{\theta_x}C_{\theta_z} & S_{\theta_x}C_{\theta_y} \\ C_{\theta_x}S_{\theta_y}C_{\theta_z} + S_{\theta_x}S_{\theta_z} & C_{\theta_x}S_{\theta_y}S_{\theta_z} - S_{\theta_x}C_{\theta_z} & C_{\theta_x}C_{\theta_y} \end{bmatrix}. \tag{72}$$

as shown on page 9 of Reference [16]. By examining the elements of the matrices in equation (71), the following relationships involving μ and γ were determined to be

$$T_{W,H}(2,3) = S_\mu C_\gamma = C_\alpha S_\beta S_\theta + C_\beta S_\phi C_\theta - S_\alpha S_\beta C_\phi C_\theta \tag{73}$$

$$T_{W,H}(3,3) = C_\mu C_\gamma = S_\alpha S_\theta + C_\alpha C_\phi C_\theta \tag{74}$$

which can be substituted into equations (69) and (70) in the gravity terms.

Additionally, the thrust force F_T terms are converted into the wind frame and expressed in terms of the vector $\begin{bmatrix} F_{T_x} & F_{T_y} & F_{T_z} \end{bmatrix}^T$, which is given in the body frame. The transformation of the F_T terms results in

$$\begin{aligned} \begin{bmatrix} F_T C_{\alpha+\alpha_T} C_\beta \\ -F_T C_{\alpha+\alpha_T} S_\beta \\ -F_T S_{\alpha+\alpha_T} \end{bmatrix} &= \begin{bmatrix} C_\alpha C_\beta & S_\beta & S_\alpha C_\beta \\ -C_\alpha S_\beta & C_\beta & -S_\alpha S_\beta \\ -S_\alpha & 0 & C_\alpha \end{bmatrix} \begin{bmatrix} F_{T_x} \\ F_{T_y} \\ F_{T_z} \end{bmatrix} \\ &= \begin{bmatrix} F_{T_x} C_\alpha C_\beta + F_{T_y} S_\beta + F_{T_z} S_\alpha C_\beta \\ -F_{T_x} C_\alpha S_\beta + F_{T_y} C_\beta - F_{T_z} S_\alpha S_\beta \\ -F_{T_x} S_\alpha + F_{T_z} C_\alpha \end{bmatrix}. \end{aligned} \tag{75}$$

Finally, the forces D, C, and L must be written in terms of the corresponding forces in the stability axes, which can be calculated directly from information in the model, as

$$\begin{aligned} \begin{bmatrix} D \\ C \\ L \end{bmatrix} &= \begin{bmatrix} C_\beta & S_\beta & 0 \\ -S_\beta & C_\beta & 0 \\ 0 & 0 & 1 \end{bmatrix} \begin{bmatrix} D_s \\ Y_s \\ L_s \end{bmatrix} \\ &= \begin{bmatrix} D_s C_\beta + Y_s S_\beta \\ -D_s S_\beta + Y_s C_\beta \\ L_s \end{bmatrix}. \end{aligned} \tag{76}$$

It is assumed that the D_s terms are absorbed into the thrust terms in equation (75).

Substituting equations (73), (74), (75), and (76) into equations (69) and (70) gives the final equations for $\dot{\beta}$ and $\dot{\alpha}$ to be

$$\dot{\beta} = \frac{1}{mV_T}\left((Y_s + F_{T_y})C_\beta + mgS_\mu C_\gamma - F_{T_x} C_\alpha S_\beta - F_{T_z} S_\alpha S_\beta\right) + (pS_\alpha - rC_\alpha) \tag{77}$$

$$\dot{\alpha} = \frac{1}{mV_T C_\beta}\left(-L_s + mgC_\mu C_\gamma - F_{T_x} S_\alpha + F_{T_z} C_\alpha\right) + (-pC_\alpha T_\beta + q - rS_\alpha T_\beta). \tag{78}$$

Now, the equation for $\dot{\mu}$ can be derived since the derivation involves the results given in equations (77) and (78). Starting from equation (57) on page 56 of Reference [12], where, for this document $\beta = -\sigma$ in Reference [12], the relationship between the angular body accelerations and the local horizon angular accelerations are expressed as

$$\begin{bmatrix} p - \dot{\beta} S_\alpha \\ q - \dot{\alpha} \\ r + \dot{\beta} C_\alpha \end{bmatrix} = \begin{bmatrix} C_\alpha C_\beta & -C_\alpha S_\beta & -S_\alpha \\ S_\beta & C_\beta & 0 \\ S_\alpha C_\beta & -S_\alpha S_\beta & C_\alpha \end{bmatrix} \begin{bmatrix} 1 & 0 & -S_\gamma \\ 0 & C_\mu & S_\mu C_\gamma \\ 0 & -S_\mu & C_\mu C_\gamma \end{bmatrix} \begin{bmatrix} \dot{\mu} \\ \dot{\gamma} \\ \dot{\chi} \end{bmatrix}. \tag{79}$$

Taking the inverse of equation (79), the equation for $\dot{\mu}$ is determined to be

$$\begin{aligned} \dot{\mu} = {} & (p - \dot{\beta} S_\alpha)\left(C_\alpha C_\beta - T_\gamma C_\alpha S_\beta S_\mu - T_\gamma S_\alpha C_\mu\right) + (q - \dot{\alpha})\left(S_\beta + T_\gamma C_\beta S_\mu\right) \\ & + (r + \dot{\beta} C_\alpha)\left(S_\alpha C_\beta + T_\gamma C_\alpha C_\mu - T_\gamma S_\alpha S_\beta S_\mu\right). \end{aligned} \tag{80}$$

Substituting equations (77) and (78) into equation (80) and simplifying gives the final equation for $\dot{\mu}$, which is

$$\begin{aligned} \dot{\mu} = \frac{1}{mV_T}\Bigg(& L_s(T_\beta + T_\gamma S_\mu) + (Y_s + F_{T_y}) T_\gamma C_\mu C_\beta - mgC_\gamma C_\mu T_\beta + (F_{T_x} S_\alpha - F_{T_z} C_\alpha)(T_\gamma S_\mu + T_\beta) \\ & - (F_{T_x} C_\alpha + F_{T_z} S_\alpha) T_\gamma C_\mu S_\beta \Bigg) + pC_\alpha \sec(\beta) + rS_\alpha \sec(\beta). \end{aligned} \tag{81}$$

Finally, equations (77), (78), and (81) are combined together in vector-matrix equation form as

$$\begin{bmatrix}\dot{\beta}\\ \dot{\alpha}\\ \dot{\mu}\end{bmatrix} = \begin{bmatrix} \frac{1}{mV_T}\left((Y_s+F_{T_y})C_\beta + mgS_\mu C_\gamma - F_{T_x}C_\alpha S_\beta - F_{T_z}S_\alpha S_\beta\right) \\ \frac{1}{mV_T C_\beta}\left(-L_s + mgC_\mu C_\gamma - F_{T_x}S_\alpha + F_{T_z}C_\alpha\right) \\ \frac{1}{mV_T}\Big(L_s(T_\beta + T_\gamma S_\mu) + (Y_s+F_{T_y})T_\gamma C_\mu C_\beta - mgC_\gamma C_\mu T_\beta \\ \quad + (F_{T_x}S_\alpha - F_{T_z}C_\alpha)(T_\gamma S_\mu + T_\beta) - (F_{T_x}C_\alpha + F_{T_z}S_\alpha)T_\gamma C_\mu S_\beta\Big) \end{bmatrix} + \begin{bmatrix} S_\alpha & 0 & -C_\alpha \\ -T_\beta C_\alpha & 1 & -T_\beta S_\alpha \\ \sec(\beta)C_\alpha & 0 & \sec(\beta)S_\alpha \end{bmatrix}\begin{bmatrix}p\\ q\\ r\end{bmatrix} \tag{82}$$

where p, q, and r are the desired angular body rates. It should be noted that it is assumed that the forces due to control surface deflections are negligible, and therefore, the force terms in equation (82) are approximated from look-up tables for the force and moment coefficients at points where the control surface deflections are equal to 0. Also, it is assumed that for the desired angular body rates that the inner loop p, q, r controller is perfect, which means that the desired angular rates equal the commanded angular rates.

Given equation (82), which is now in the form of equation (1), the adaptive dynamic inversion controller can be constructed using equations (5) and (13).

VI. Robustness Analysis

Based on the control and adaptive laws derived in the previous sections, a simulation of the entire GHV system with the nonlinear adaptive nonlinear dynamic inversion control architecture was created in Simulink. In order to make the simulation more realistic, second-order actuator dynamics with damping ratio $\zeta = 0.7$ and natural frequency $\omega_n = 25$ Hz are included in the current simulation, and position and rate limits are placed on the control surfaces of 30 deg and 100 deg/s, respectively. Additionally, a time delay of 0.03 s is included in the simulation; however, it should be noted that the simulation can tolerate time delays of up to 0.04 s without the responses becoming significantly oscillatory. Commands to α, β, and μ are given as ramp signals from 0 degrees to a commanded angle in fixed time. For the α, β, μ inversion controller, the basis function $\beta(x;d)$ is chosen to be $\beta(x;d) = \begin{bmatrix} c & \alpha & \beta & \mu & M \end{bmatrix}^T$, where c is a constant bias term. For the p, q, r inversion controller, the basis function $\beta(x;d)$ is chosen to be $\beta(x;d) = \begin{bmatrix} c & p & q & r & \alpha & \beta & M \end{bmatrix}^T$, where c is a constant bias term.

The total velocity of the vehicle is controlled using a PID controller, which is not depicted in Figure 2. The input to the controller is the commanded total velocity of the GHV, and the output of the controller is the equivalence ratio. The equivalence ratio is the fifth control, and along with the four control surfaces, completes the the control complement for the vehicle. Additionally, a saturation limiter has been added after the velocity PID controller to constrain the equivalence ratio to be between 0 and 1.

In the derivation of the adaptive dynamic controllers in Section III, a reference model was described. The difference between this reference model and the actual system dynamics constitutes the tracking error of the system. In order to determine the reference states of the system, the reference signal r must be defined. For the α, β, μ inversion controller, the reference signal consists of the commanded values of α, β, and μ. For the p, q, r inversion controller, the reference signal consists of the commanded angular body rates from the α, β, μ inversion controller. Both of the reference models have the general form

$$\begin{bmatrix}\dot{x}_1\\ \dot{x}_2\\ \dot{x}_3\end{bmatrix} = \begin{bmatrix}\xi_1 & 0 & 0\\ 0 & \xi_2 & 0\\ 0 & 0 & \xi_3\end{bmatrix}\begin{bmatrix}x_1\\ x_2\\ x_3\end{bmatrix} + \begin{bmatrix}\eta_1 & 0 & 0\\ 0 & \eta_2 & 0\\ 0 & 0 & \eta_3\end{bmatrix}\begin{bmatrix}r_1\\ r_2\\ r_3\end{bmatrix} \tag{83}$$

where $\xi_1, \xi_2, \xi_3, \eta_1, \eta_2,$ and η_3 are scalars that define the desired time constants of each control channel.

The open-loop poles of the linearized dynamics at the flight condition of Mach 6 at 80,000 ft for both the longitudinal and lateral-directional states are shown in Figure 3. It should be noted from the eigenvalues

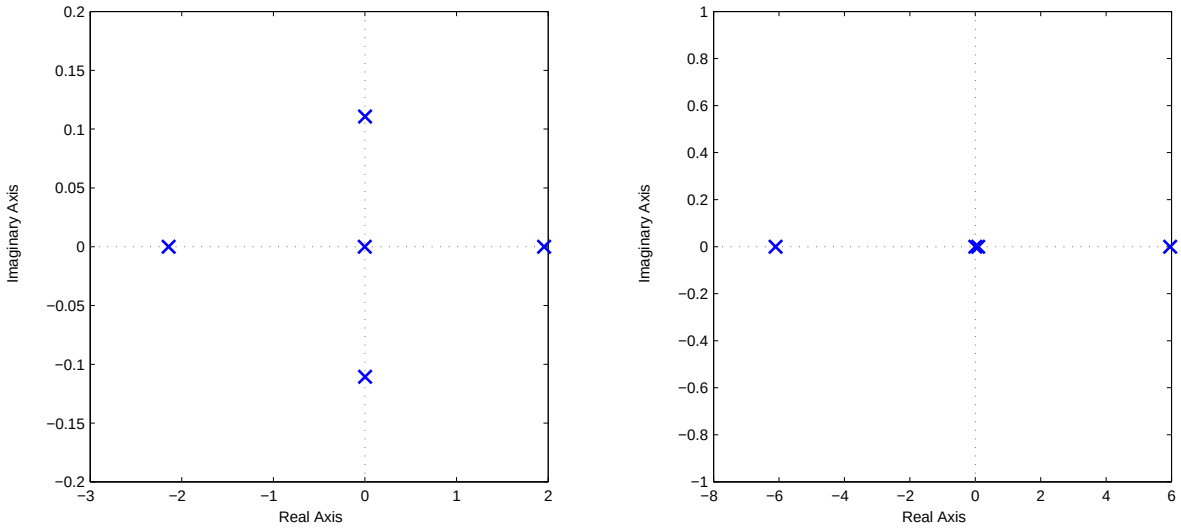

(a) Longitudinal.

(b) Lateral/Directional.

Figure 3. Open-loop poles for the linearized longitudinal and lateral/directional dynamics.

Table 1. Eigenvalues for the linearized longitudinal dynamics.

Eigenvalue	Damping Ratio	Natural Frequency (rad/s)
-2.14	1.00	2.14
-2.79×10^{-3}	1.00	2.79×10^{-3}
$1.25 \times 10^{-3} \pm 0.111j$	-0.0113	0.111
1.96	-1.00	1.96

Table 2. Eigenvalues for the linearized lateral/directional dynamics.

Eigenvalue	Damping Ratio	Natural Frequency (rad/s)
-6.10	1.00	6.10
2.22×10^{-16}	-1.00	2.22×10^{-16}
0.088	-1.00	0.088
5.96	-1.00	5.96

listed in Tables 1 and 2 that both the longitudinal and lateral-directional states have several eigenvalues in the right-half plane, which indicates that the GHV is an unstable vehicle. A nonlinear adaptive dynamic inversion controller will be able to suppress the unstable dynamics and replace them with desired dynamics for the aircraft.

Figures 4 and 5 show representative simulation results with the nonlinear adaptive dynamic inversion control architecture for the commands $\alpha = \pm 2$ deg, $\beta = 0$ deg, and $\mu = 70$ deg. The responses are well-behaved, and the control architecture is able to achieve the desired tracking performance without excessive control effort.

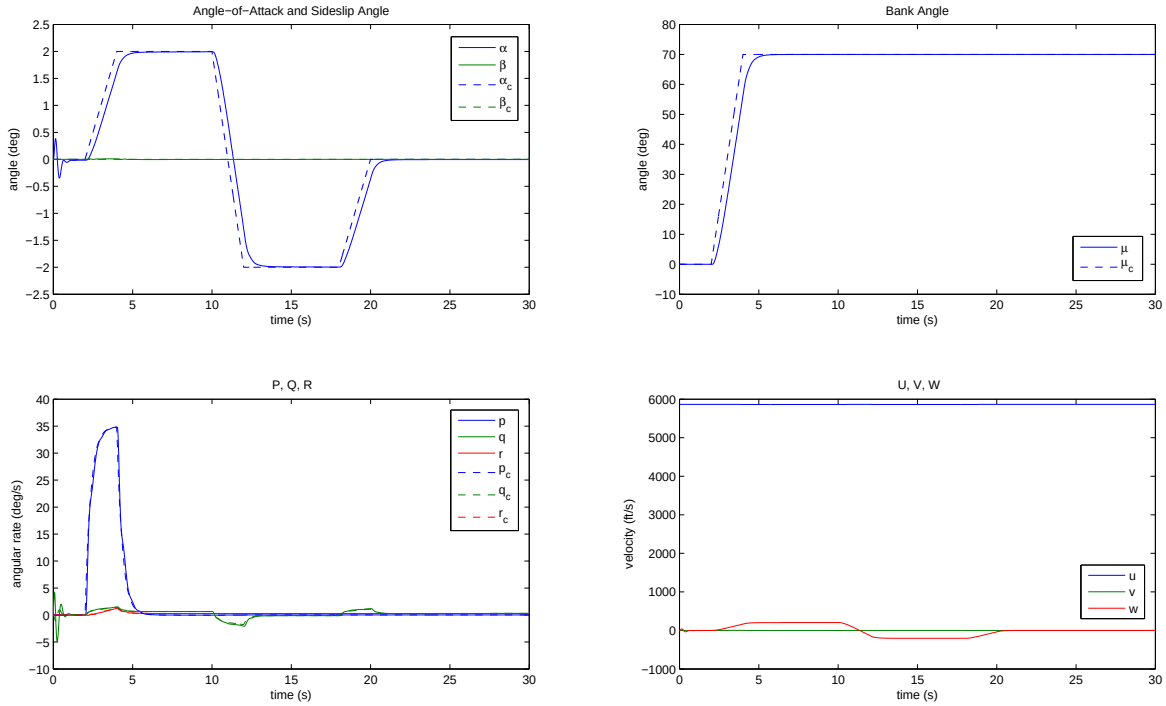

Figure 4. State responses for the commands $\alpha = \pm 2$ deg, $\beta = 0$ deg, and $\mu = 70$ deg.

A robustness analysis was performed via simulation on the designed adaptive nonlinear dynamic inversion control architecture from the previous section in order to determine the maximum tolerable uncertainties in selected parameters for the control architecture. Uncertainties in the plant examined in the analysis include the additive uncertainties ΔC_{m_α}, ΔC_{n_β}, and ΔC_m and multiplicative gains D on the control surface deflections, given in terms of equations as

$$C_m = C_{m_{baseline}} + \Delta C_{m_\alpha} \alpha \tag{84}$$

$$C_n = C_{n_{baseline}} + \Delta C_{n_\beta} \beta \tag{85}$$

$$C_m = C_{m_{baseline}} + \Delta C_m \tag{86}$$

$$C_\delta = D C_{\delta_o}. \tag{87}$$

The criteria for determining the bounds on the uncertainties is that the states must not demonstrate oscillatory behavior.

Tables 3 and 4 provide the maximum and minimum values of the additive uncertainties ΔC_{m_α} and ΔC_{n_β} for various α, β, and μ commands. It should be noted that an examination of the maximum and minimum baseline values of C_{m_α} and C_{n_β} show that these values are on the order of 10^{-4}, which is typical of a high-speed vehicle. The maximum and minimum values for ΔC_{m_α} and ΔC_{n_β} in Tables 3 and 4 are on the order of $10^{-4} - 10^{-3}$, and therefore, the control architecture is able to withstand considerable uncertainties

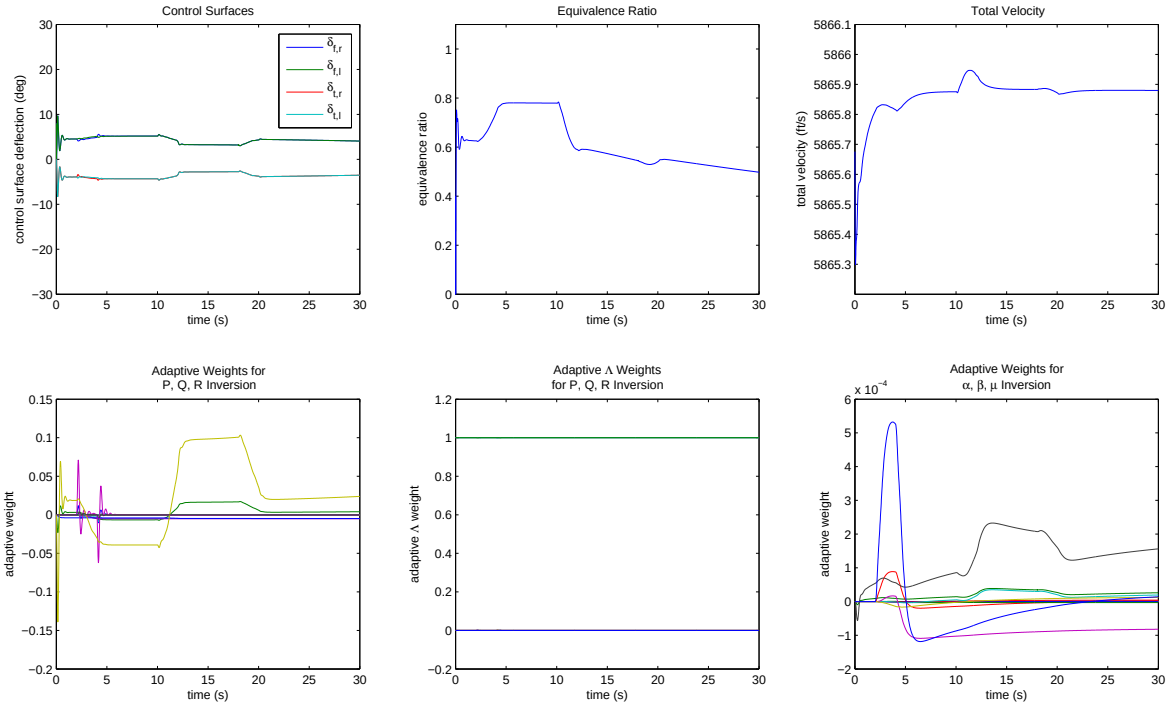

Figure 5. Control and adaptive weight responses for the commands $\alpha = \pm 2$ deg, $\beta = 0$ deg, and $\mu = 70$ deg.

in C_{m_α} and C_{n_β} and maintain stable tracking flight. Similar results for the additive uncertainty ΔC_m can be found in Table 5.

Table 6 contains the minimum allowable multiplicative gains D on the control surface deflections for various α, β, and μ commands. These gains represent a loss of control effectiveness for one or more of the control surfaces on the GHV. For all cases, the vehicle is able to tolerate low values of control effectiveness, which shows that the control architecture is robust to loss of control effectiveness.

Table 3. Additive uncertainty ΔC_{m_α} over a 30 s period with 0.03 s time delay.

α (deg)	β (deg)	μ (deg)	max ΔC_{m_α} (deg^{-1})	min ΔC_{m_α} (deg^{-1})
5	0	0	0.0005	-0.0013
5	1	20	0.0003	-0.0011

It should be noted that following this preliminary analysis of the nonlinear adaptive dynamic inversion control architecture, pseudo-control hedging ([17],[18]) was added to the simulation in order to protect the nonlinear adaptive dynamic inversion control architecture during periods of control surface saturation. However, for most of the cases simulated for the GHV for this paper, control surface saturation was not encountered.

VII. Reference Trajectory Generation

While the tracking of α, β, and μ was achieved as demonstrated in Section VI, it was desired that the GHV have the ability to track a realistic trajectory instead of selected commands. In order to control flight path angle γ as opposed to α, a nonzero setpoint (NZSP) controller ([19], [20]) was designed to generate

Table 4. Additive uncertainty ΔC_{n_β} over a 30 s period with 0.03 s time delay.

α (deg)	β (deg)	μ (deg)	max ΔC_{n_β} (deg^{-1})	min ΔC_{n_β} (deg^{-1})
0	1	0	0.007	-0.003
5	0	20	0.01	-0.004
5	1	20	0.006	-0.003

Table 5. Additive uncertainty ΔC_m over a 30 s period with 0.03 s time delay.

α (deg)	β (deg)	μ (deg)	max ΔC_m	min ΔC_m
5	0	0	0.0005	-0.003
5	1	20	0.0005	-0.002

Table 6. Multiplicative gains D on control surface deflection terms over a 30 s period with 0.03 s time delay.

α (deg)	β (deg)	μ (deg)	$D_{\delta_{f,r}}$	$D_{\delta_{f,l}}$	$D_{\delta_{t,r}}$	$D_{\delta_{t,l}}$
5	0	0	1	0.14	1	1
5	0	0	1	1	1	0.01
5	0	0	0.15	0.15	1	1
5	0	0	1	1	0.15	0.15
5	0	20	1	0.31	1	1
5	0	20	1	1	1	0.01
5	0	20	0.21	0.21	1	1
5	0	20	1	1	0.30	0.30
5	1	20	1	0.42	1	1
5	1	20	1	1	1	0.05
5	1	20	0.38	0.38	1	1
5	1	20	1	1	0.38	0.38

trajectories for the GHV to follow. The NZSP controller requires a linear model, so the nonlinear GHV plant model was linearized about a flight condition specified by the Mach number and altitude. Assuming that the vehicle remains wings-level during its flight of the trajectory, only the longitudinal dynamics model will be required for the trajectory generation. For the NZSP controller, the longitudinal states are $\begin{bmatrix} u & \theta & q & \alpha \end{bmatrix}^T$, and the controls are $\begin{bmatrix} \delta_T & \delta_e \end{bmatrix}^T$ where δ_T represents the equivalence ratio control, and δ_e represents the elevator control, expressed in terms of the GHV controls as $\delta_e = (\delta_{f,r} + \delta_{f,l})/2$. The outputs y_m to be commanded by the NZSP controller are velocity u and flight path angle γ, which can be expressed in matrix-vector form as

$$y_m = \begin{bmatrix} u \\ \gamma \end{bmatrix} = \begin{bmatrix} 1 & 0 & 0 & 0 \\ 0 & -1 & 0 & 1 \end{bmatrix} \begin{bmatrix} u \\ \theta \\ q \\ \alpha \end{bmatrix} + \begin{bmatrix} 0 & 0 \\ 0 & 0 \end{bmatrix} \begin{bmatrix} \delta_T \\ \delta_e \end{bmatrix}. \tag{88}$$

By fitting a polynomial to the trajectory generated for γ, and finding the derivative of that polynomial, the reference model for γ is completely defined for the GHV simulation. In order to implement the γ, β, μ inversion controller, the dynamic equation for $\dot{\gamma}$ must be derived and written in the form of equation (1) as

$$\dot{\gamma} = f(s) + g(s) \begin{bmatrix} p \\ q \\ r \end{bmatrix} \tag{89}$$

where s represents the states in the GHV simulation. The equation for $\dot{\gamma}$ is derived using the same process that was applied to find $\dot{\mu}$ in Section V. Starting from equation (79), and taking its inverse, the equation for $\dot{\gamma}$ is determined to be

$$\dot{\gamma} = D(p - \dot{\beta}S_\alpha) + E(q - \dot{\alpha}) + F(r + \dot{\beta}C_\alpha) \tag{90}$$

where

$$D = C_\alpha S_\beta C_\mu - S_\alpha S_\mu \tag{91}$$

$$E = C_\beta C_\mu \tag{92}$$

$$F = \frac{{C_\alpha}^2 S_\beta {C_\mu}^2 - C_\alpha S_\alpha \left({S_\beta}^2 + 1\right) C_\mu S_\mu + \left({S_\alpha}^2 {S_\mu}^2 - 1\right) S_\beta}{C_\alpha S_\beta S_\mu + S_\alpha C_\mu}. \tag{93}$$

Consider the equations for $\dot{\beta}$ and $\dot{\alpha}$ in equations (77) and (78), respectively to have the following form

$$\dot{\beta} = f_\beta + (pS_\alpha - rC_\alpha) \tag{94}$$

$$\dot{\alpha} = f_\alpha + (-pC_\alpha T_\beta + q - rS_\alpha T_\beta) \tag{95}$$

where f_β and f_α represent the terms in $\dot{\beta}$ and $\dot{\alpha}$, respectively, that do not depend explicitly on the angular rates p, q, and r. Substituting equations (94) and (95) into equation (90) and simplifying the expression gives the resulting equation for $\dot{\gamma}$ that

$$\begin{aligned} \dot{\gamma} = & -Df_\beta S_\alpha - Ef_\alpha + Ff_\beta C_\alpha \\ & + p\left(D - D{S_\alpha}^2 + EC_\alpha T_\beta + FC_\alpha S_\alpha\right) \\ & + q\,(0) \\ & + r\left(DC_\alpha S_\alpha + ES_\alpha T_\beta + F - F{C_\alpha}^2\right). \end{aligned} \tag{96}$$

Note that there is no dependence on q in the equation for $\dot{\gamma}$. Consequently, when the dynamic equations for β, γ, and μ are expressed in the form

$$\begin{bmatrix} \dot{\beta} \\ \dot{\gamma} \\ \dot{\mu} \end{bmatrix} = f(s) + g(s) \begin{bmatrix} p \\ q \\ r \end{bmatrix} \tag{97}$$

where s represents the states of the GHV, the resulting expression for g(s) is

$$g(s) = \begin{bmatrix} S_\alpha & 0 & -C_\alpha \\ \left(D - D{S_\alpha}^2 + EC_\alpha T_\beta + FC_\alpha S_\alpha\right) & 0 & \left(DC_\alpha S_\alpha + ES_\alpha T_\beta + F - F{C_\alpha}^2\right) \\ \sec(\beta)C_\alpha & 0 & \sec(\beta)S_\alpha \end{bmatrix}. \tag{98}$$

As can be seen in equation (98), $g(s)$ is not invertible, which causes a problem with the computation of p, q, and r in the new γ, β, μ inversion block. If $g(s)$ cannot be inverted, then the commands for p, q, and r cannot be determined for the inversion controller. Therefore, substituting the equation for $\dot{\gamma}$ for the equation for $\dot{\alpha}$ in the α, β, μ inversion controller in order to track a trajectory for γ is not possible for the GHV simulation, and another method of including the γ trajectory in the GHV simulation had to be determined.

In order to allow for the GHV simulation to track a flight path angle trajectory, a method from Reference [21] was applied in which the equation for $\ddot{h}$, where h represents the altitude of the aircraft, is written in the form

$$\ddot{h} = f_h(s) + g_h(s) \begin{bmatrix} p \\ q \\ r \end{bmatrix}. \tag{99}$$

Given the equation for $\dot{h}$

$$\dot{h} = V\left(C_\beta C_\alpha S_\theta - S_\beta S_\phi C_\theta - C_\beta S_\alpha C_\phi C_\theta\right), \tag{100}$$

where V is the total velocity of the vehicle, the equation for $\ddot{h}$ is determined to be

$$\ddot{h} = \left[b_0\dot{V} + b_1\dot{\beta} + b_2\dot{\alpha}\right] + \begin{bmatrix} a_0 & a_1 & a_2 \end{bmatrix} \begin{bmatrix} p \\ q \\ r \end{bmatrix} \tag{101}$$

where

$$\begin{aligned} a_0 &= b_4 \\ a_1 &= b_3 C_\phi + b_4 S_\phi T_\theta \\ a_2 &= b_4 C_\phi T_\theta - b_3 S_\phi \end{aligned}$$

and

$$\begin{aligned} b_0 &= C_\beta C_\alpha S_\theta - S_\beta S_\phi C_\theta - C_\beta S_\alpha C_\phi C_\theta \\ b_1 &= V\left(-S_\beta C_\alpha S_\theta - C_\beta S_\phi C_\theta + S_\beta S_\alpha C_\phi C_\theta\right) \\ b_2 &= V\left(-C_\beta S_\alpha S_\theta - C_\beta C_\alpha C_\phi C_\theta\right) \\ b_3 &= V\left(C_\beta C_\alpha C_\theta + S_\beta S_\phi S_\theta + C_\beta S_\alpha C_\phi S_\theta\right) \\ b_4 &= V\left(-S_\beta C_\phi C_\theta + C_\beta S_\alpha S_\phi C_\theta\right). \end{aligned}$$

Because $\ddot{h}$ has a nonzero coefficient for q, which means that the term $g(s)$ in equation (97) is invertible, the equation for $\ddot{h}$ can replace the equation for $\dot{\alpha}$ in equation (82) for the α, β, μ inversion controller. The original reference trajectory that is generated for γ using the NZSP controller can be converted to $\dot{h}$ using the relation from aircraft kinematics that $\dot{h} = VS_\gamma$. Once a polynomial is fitted to the new trajectory for $\dot{h}$, and the derivative of that polynomial is determined, the reference model is defined for $\dot{h}$. The $\dot{h}$, β, μ inversion controller replaces the original α, β, μ inversion controller in the GHV simulation, and now desired trajectories for γ can be tracked.

VIII. Simulation Results

The GHV simulation with the $\dot{h}$, β, μ inversion controller was implemented in Simulink. A trajectory for γ was generated at the flight condition of Mach 6 at 80,000 ft. Figures 6, 7, and 8 present representative simulation results for the flight path angle trajectory shown in Figure 6. It should be noted that in this particular simulation, a command of $\beta = -4^o$ also is given to the GHV. The nonlinear adaptive dynamic inversion control architecture achieves the desired tracking performance for the generated flight path angle trajectory and sideslip angle.

A simplified inlet unstart model was added to test the ability of the nonlinear adaptive dynamic inversion control architecture to handle tracking a trajectory during an inlet unstart. For the simulation, an inlet unstart is triggered at a specified time, and the loss of thrust and changes to aerodynamic parameters following the unstart are modeled as instantaneous changes. The coefficient of the axial force (C_A) is increased slightly, and the coefficient of the normal force (C_N) is decreased slightly. Additive variations in C_{m_α} and C_{n_β} are included in the plant through the equations

$$C_m = C_{m_{baseline}} + \Delta C_{m_\alpha}\alpha \tag{102}$$

$$C_n = C_{n_{baseline}} + \Delta C_{n_\beta}\beta. \tag{103}$$

Through a robustness analysis, it was determined that the maximum destabilizing additive variations in C_{m_α} and C_{n_β} that the nonlinear adaptive dynamic inversion control architecture could tolerate were $\Delta C_{m_\alpha} = 0.001$ deg^{-1} and $\Delta C_{n_\beta} = -0.001$ deg^{-1}.

Figures 9, 10, and 11 show the results for the GHV simulation during flight path angle tracking with an inlet unstart that occurs at time t = 10 seconds. It should be noted in Figure 11 that while the equivalence ratio is commanded to its maximum value following the inlet unstart, thrust is not being generated by the vehicle after time t = 10 seconds. While tracking performance is somewhat degraded, the aircraft is still able to nominally track the specified flight path angle trajectory.

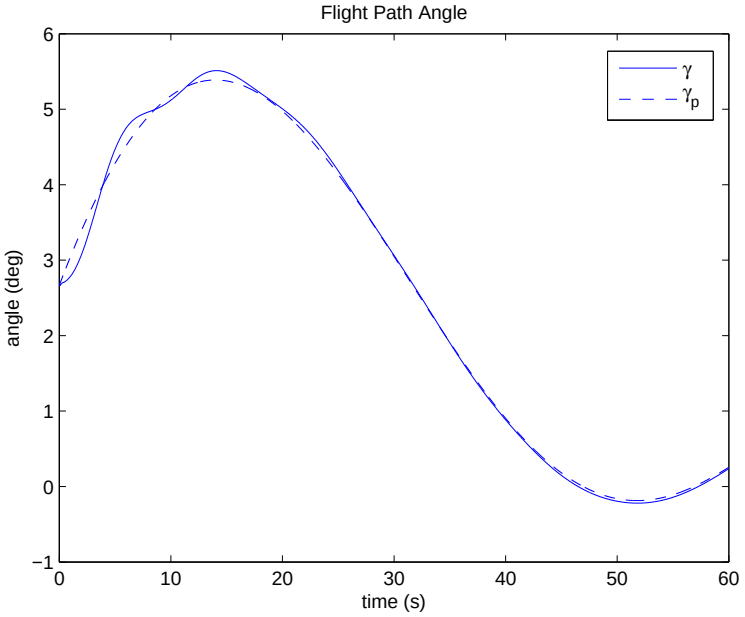

Figure 6. Flight path angle response compared with the generated flight path angle trajectory. The subscript p represents the flight path angle computed from the polynomial fit of $\dot{h}$.

IX. Conclusions

Because the dynamic equations for the GHV are inherently nonlinear and the aerodynamic and control derivatives for the aircraft have significant uncertainty associated with them, a nonlinear adaptive dynamic inversion control architecture was selected as the preferred control architecture to stabilize and control the aircraft. Based on the simulation results and the robustness analysis, it can be seen that the objective of designing a control architecture that is robust in order to achieve desired tracking performance was achieved for the GHV. The control architecture is robust to decreases in control surface effectiveness, changes in system parameters, and time delays of 0.04 s or less. The responses for tracking generated flight-path angle trajectories are well behaved, and the necessary control effort for tracking is not excessive. Additionally, the control architecture is able to tolerate an inlet unstart and maintain nominal tracking of a specified flight

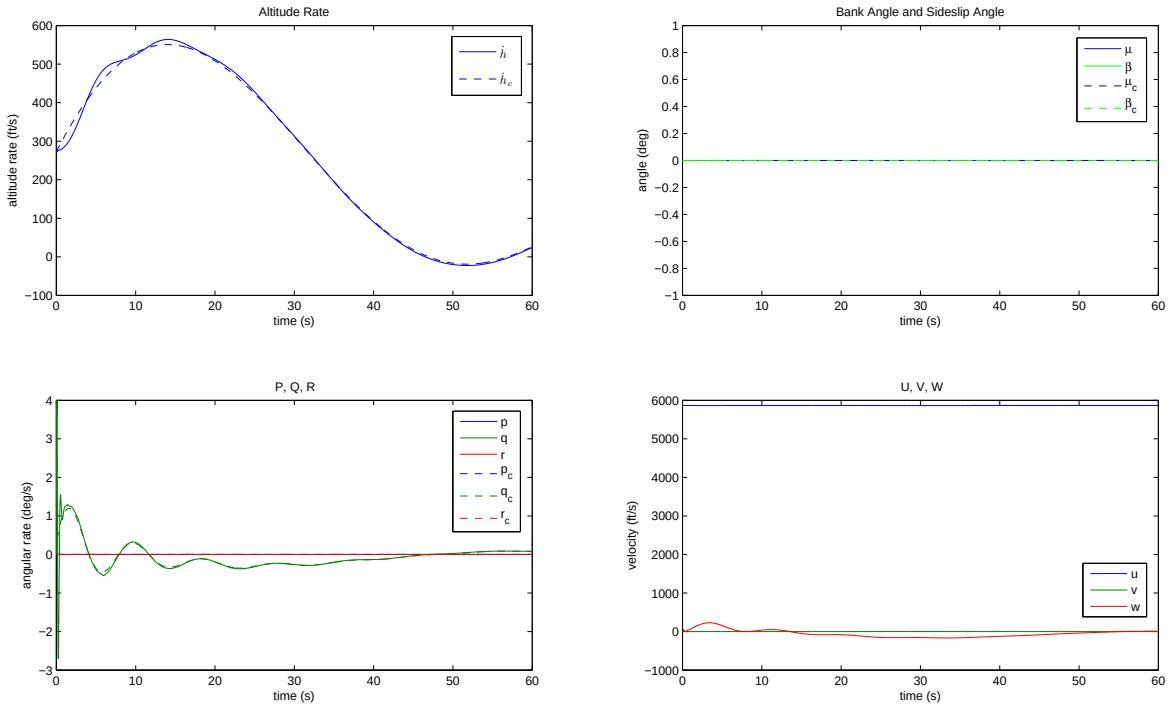

Figure 7. State responses for the generated flight path angle trajectory.

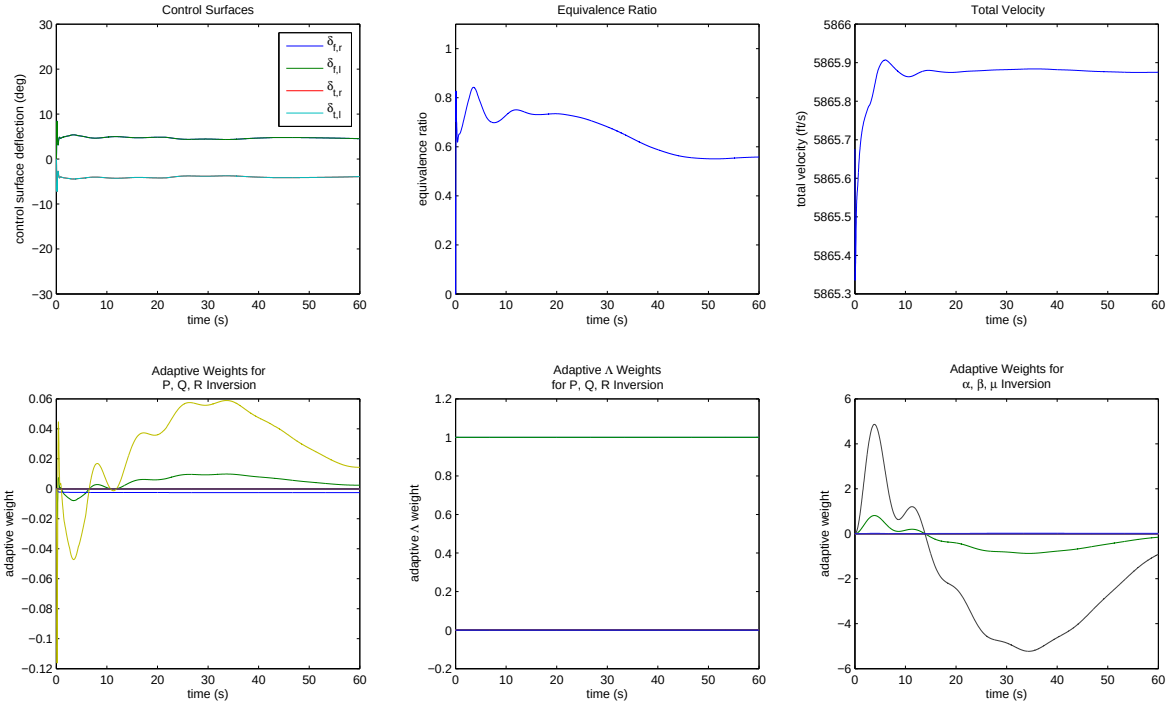

Figure 8. Control and adaptive weight responses for the generated flight path angle trajectory.

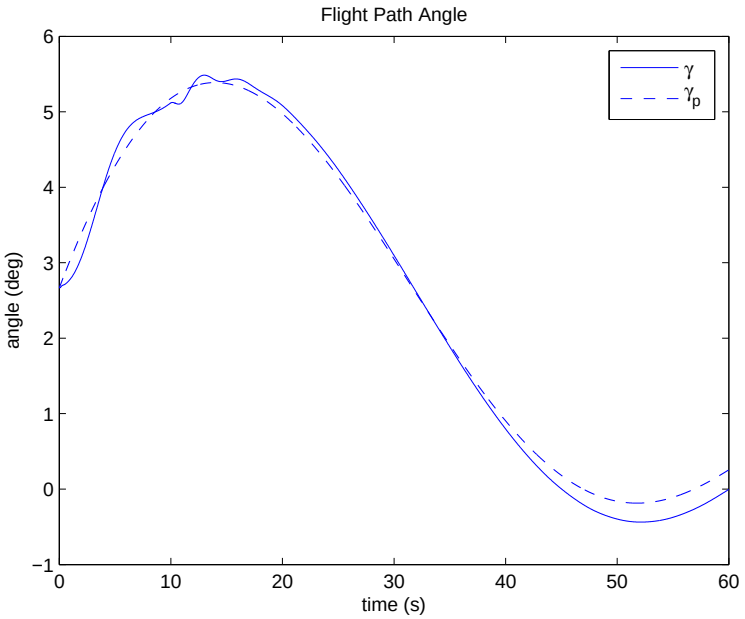

Figure 9. Flight path angle response compared with the generated flight path angle trajectory during an inlet unstart. The subscript p represents the flight path angle computed from the polynomial fit of $\dot{h}$.

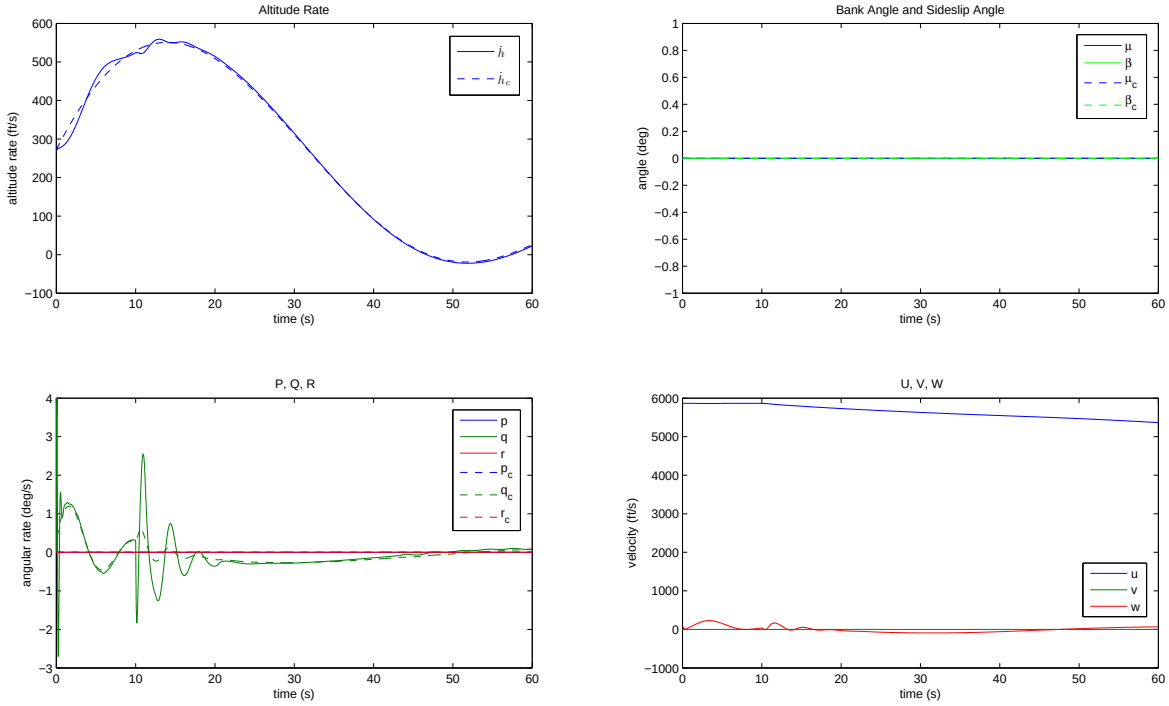

Figure 10. State responses for the generated flight path angle trajectory during an inlet unstart.

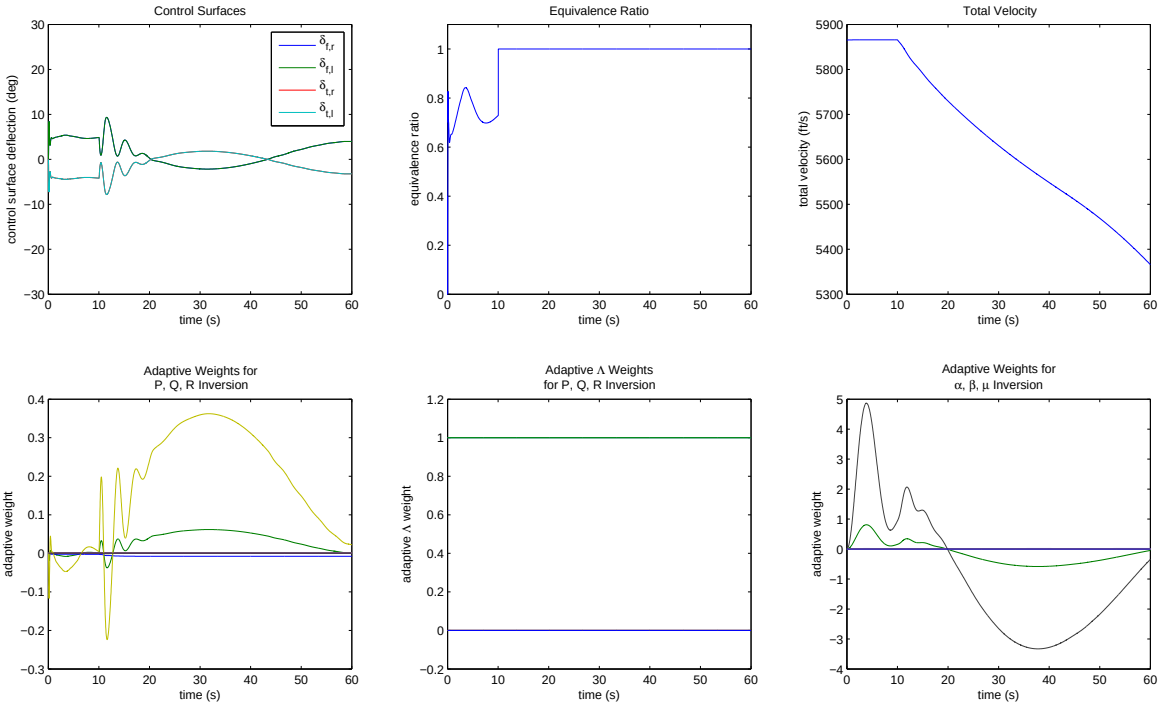

Figure 11. Control and adaptive weight responses for the generated flight path angle trajectory during an inlet unstart.

path angle trajectory. Therefore, it can be concluded that this approach of nonlinear adaptive dynamic inversion control works well as a control architecture for the GHV.

Acknowledgements

This research was funded in part by the Air Force Research Laboratory/Air Vehicles Directorate Summer Researcher Program. The author gratefully acknowledges this support. Approved for Public Release; Distribution Unlimited. Case Number 88ABW-2013-3391.

References

[1]Heiser, W. H. and Pratt, D. T., *Hypersonic Airbreathing Propulsion*, AIAA Education Series, American Institute of Aeronautics and Astronautics, Washington D. C., 1994.

[2]Annaswamy, A. M., Jang, J., and Lavretsky, E., "Adaptive gain-scheduled controller in the presence of actuator anomalies," *AIAA Guidance, Navigation and Control Conference and Exhibit*, Honolulu, Hawaii, August 2008.

[3]Gibson, T. E. and Annaswamy, A. M., "Adaptive Control of Hypersonic Vehicles in the Presence of Thrust and Actuator Uncertainties," *AIAA Guidance, Navigation and Control Conference and Exhibit*, Honolulu, Hawaii, August 2008.

[4]Groves, K. P., Sigthorsson, D. O., Serrani, A., Yurkovich, S., Bolender, M. A., and Doman, D. B., "Reference Command Tracking for a Linearized Model of an Air-breathing Hypersonic Vehicle," *AIAA Guidance, Navigation and Control Conference and Exhibit*, San Francisco, California, August 2005.

[5]Bolender, M. A., Staines, J. T., and Dolvin, D. J., "HIFiRE 6: An Adaptive Flight Control Experiment," *50th AIAA Aerospace Sciences Meeting including the New Horizons Forum and Aerospace Exposition*, Nashville, TN, January 2012.

[6]Johnson, E. N., Calise, A. J., Curry, M. D., Mease, K. D., and Corban, J. E., "Adaptive Guidance and Control for Autonomous Hypersonic Vehicles," *Journal of Guidance, Control, and Dynamics*, Vol. 29, No. 3, May-June 2006, pp. 725–737.

[7]Fiorentini, L., Serrani, A., Bolender, M. A., and Doman, D. B., "Nonlinear Robust Adaptive Control of Flexible Air-breathing Hypersonic Vehicles," *Journal of Guidance, Control, and Dynamics*, Vol. 32, No. 2, Mar.-Apr. 2009, pp. 401–416.

[8]Parker, J. T., Serrani, A., Yurkovich, S., Bolender, M. A., and Doman, D. B., "Approximate Feedback Linearization of an Air-breathing Hypersonic Vehicle," *AIAA Guidance, Navigation and Control Conference and Exhibit*, Keystone, Colorado, August 2006.

[9]Parker, J. T., Serrani, A., Yurkovich, S., Bolender, M. A., and Doman, D. B., "Control-Oriented Modeling of an Air-Breathing Hypersonic Vehicle," *Journal of Guidance, Control, and Dynamics*, Vol. 30, No. 3, May-June 2007, pp. 859–869.

[10]Snell, S. A., Enns, D. F., and Garrard Jr., W. L., "Nonlinear Inversion Flight Control for a Supermaneuverable Aircraft," *AIAA Guidance, Navigation, and Control Conference Technical Papers*, Vol. Part 1, American Institute of Aeronautics and Astronautics, Washington D. C., August 1990, pp. 808–825.

[11]Vick, T. J., "Documentation for Generic Hypersonic Vehicle Model," Tech. rep., U.S. Air Force Research Laboratory, Wright-Patterson AFB.

[12]Miele, A., *Flight Mechanics*, Vol. 1: Theory of Flight Paths, Addison-Wesley Publishing Company, Inc., Reading, 1962.

[13]Pomet, J.-B. and Praly, L., "Adaptive Nonlinear Regulation: Estimation from the Lyapunov Equation," *IEEE Transactions on Automatic Control*, Vol. 37, No. 6, June 1992, pp. 729–740.

[14]Slotine, J.-J. E. and Li, W., *Applied Nonlinear Control*, Prentice Hall, Inc., Upper Saddle River, 1991.

[15]Stevens, B. L. and Lewis, F. L., *Aircraft Control and Simulation*, Wiley, Hoboken, 2nd ed., 2003.

[16]Schmidt, D. K., *Modern Flight Dynamics*, McGraw-Hill, New York, 2012.

[17]Johnson, E. N., *Limited Authority Adaptive Flight Control*, Ph.D. thesis, Georgia Institute of Technology, November 2000.

[18]Johnson, E. N. and Kannan, S. K., "Adaptive Flight Control for an Autonomous Unmanned Helicopter," *AIAA Guidance, Navigation and Control Conference and Exhibit*, Monterey, California, August 2002.

[19]Valasek, J., "Optimal Setpoint Controller for a Generic X-29A Aircraft with Forebody Vortex Nozzles," *Proceedings of the 1996 IEEE International Conference on Control Applications*, Dearborn, Michigan, September 1996.

[20]Stengel, R. F., *Stochastic Optimal Control: Theory and Applications*, Wiley, New York, 1986.

[21]Menon, P., Badgett, M., Walker, R., and Duke, E., "Nonlinear Flight Test Trajectory Controllers for Aircraft," *Journal of Guidance, Control, and Dynamics*, Vol. 10, No. 1, Jan.-Feb. 1987, pp. 67–72.